LASER INTERFEROMETER GRAVITATIONAL WAVE OBSERVATORY
- LIGO -
CALIFORNIA INSTITUTE OF TECHNOLOGY
MASSACHUSETTS INSTITUTE OF TECHNOLOGY

Technical Note	**LIGO-T2400254-x-0**	Wednesday 21 August, 2024

LIGO SURF 2024:Interim Report II — Vacuum Beam Guide for Quantum Communication

Prakhar Maheshwari

California Institute of Technology
LIGO Project, MS 18-34
Pasadena, CA 91125
Phone (626) 395-2129
Fax (626) 304-9834
E-mail: info@ligo.caltech.edu

Massachusetts Institute of Technology
LIGO Project, Room NW22-295
Cambridge, MA 02139
Phone (617) 253-4824
Fax (617) 253-7014
E-mail: info@ligo.mit.edu

LIGO Hanford Observatory
Route 10, Mile Marker 2
Richland, WA 99352
Phone (509) 372-8106
Fax (509) 372-8137
E-mail: info@ligo.caltech.edu

LIGO Livingston Observatory
19100 LIGO Lane
Livingston, LA 70754
Phone (225) 686-3100
Fax (225) 686-7189
E-mail: info@ligo.caltech.edu

http://www.ligo.caltech.edu/

Contents

1 Introduction

Quantum communication is poised to become a fundamental technology for future data transmission, requiring efficient solutions for long-distance communication on a continental scale[1]. While optical fiber cables have revolutionized traditional communication, they present significant photon loss challenges, with absorption rates around 0.1 dB per kilometer[3]. This loss is particularly problematic for quantum communication systems[5], especially those utilizing continuous-variable quantum communication, where loss is a critical parameter to manage.

For instance, in optical squeezing, losses cap the maximum achievable squeezing levels. As detailed in the supplementary materials of [2] by Goodwin-Jones et al., the relationship between squeezing and loss is given by:

$$S = S_0(1 - l) + l, \tag{1}$$

where S_0 represents the initial ratio of squeezing to vacuum variance, S is the ratio after loss, and l denotes the fractional power loss in the system.

To mitigate these challenges, two primary strategies have been proposed: satellite-based communication and quantum repeaters. Nicolas Sangouard and colleagues explore a quantum repeater approach using atomic ensembles as quantum memories[7]. Meanwhile, Sumit Goswami et al. propose a network of low Earth orbit (LEO) satellites with total estimated losses of less than 30 dB over 20,000 km, equating to approximately 0.001 dB/km. This system assumes that each satellite, separated by 120 km, maintains other losses below 2% and employs 60-cm diameter telescopes to minimize diffraction loss[8].

An innovative approach presented by Yuexun et al.[5] involves a vacuum beam guide (VBG). This method uses an array of lenses to guide light through a vacuum pipe, enabling long-range quantum communication over thousands of kilometers with a quantum channel capacity exceeding 10^{13} qubits/sec. Using this methodology, photon losses can be limited to approximately 0.0001 dB/km, making it the most efficient method for long-distance quantum communication. Photon losses in the VBG arise from three factors: lens losses, residual gas absorption, and imperfect alignment, collectively represented as[5]:

$$\alpha_{\text{total}} = \alpha_{\text{lens}} + \alpha_{\text{gas}} + \alpha_{\text{align}} \tag{2}$$

Lens loss, denoted as α_{lens}, results from absorption, scattering, reflection, and diffraction. Proper lens radius selection minimizes diffraction loss, and multi-layer anti-reflective coatings reduce lens losses to less than 0.0001 dB/km at wavelengths around 1550 nm. Gas loss within the VBG, primarily due to absorption by residual air at 1 Pascal pressure, also remains below 0.0001 dB/km at similar wavelengths. Imperfect alignment in the confocal design contributes to the effective attenuation rate, expressed as[5]:

$$\alpha_{\text{align}} \leq \frac{-10}{L_0} \log_{10}\left(1 - \frac{2\sigma^2}{w_0^2} - \frac{\sigma^2 L_0}{L_0^2} - \frac{\sigma^2 f}{f^2}\right) \tag{3}$$

where σ_s and σ_{L_0} represent transverse and longitudinal displacement fluctuations, respectively, and σ_f indicates focal length deviation.

Progress has been made toward optimizing the parameters of a lens array to minimize photon losses. The primary parameters under investigation include the focal length/focal scale, lens separation (L_{Lens}), and the initial beam parameter q. For simplicity, the lens separation (the distance between any two adjacent lenses) is assumed to be uniform across the entire array. Additionally, the initial beam parameter is optimized as two distinct parameters: w_0 and z_0, representing the beam waist and Rayleigh range, respectively, for the starting point of the beam.

2 Optimization to get the best parameters

The differential evolution algorithm was employed to achieve the optimal set of parameters. This algorithm effectively searches for the best parameters to minimize losses. In the initial findings, we searched for optimal parameters for a lens radius of 12 cm and 14 cm of lens. A serrated aperture was introduced into the model to further understand the impact of scattering.

2.1 Differential Evolution Algorithm

The Differential Evolution (DE) algorithm is a powerful stochastic optimization method used for solving multidimensional continuous optimization problems. It was introduced by Storn and Price in 1995 and has since been widely applied in various fields due to its simplicity, efficiency, and robustness [6]. The algorithm operates through a population-based approach, iteratively improving candidate solutions based on the principles of mutation, crossover, and selection.

Initialization In the initialization step, a population of N_p candidate solutions, also known as individuals, is randomly generated. Each individual is a vector in the search space, typically represented as $\mathbf{x}_{i,G}$ for the i-th individual in the G-th generation. The initial population is created within the defined parameter bounds:

$$x_{i,j,0} = x_{j,\min} + \text{rand}_j(0,1) \cdot (x_{j,\max} - x_{j,\min})$$

where $x_{i,j,0}$ is the j-th parameter of the i-th individual, $x_{j,\min}$ and $x_{j,\max}$ are the lower and upper bounds of the j-th parameter, and $\text{rand}_j(0,1)$ is a uniformly distributed random number between 0 and 1.

Mutation Mutation is the process of creating a mutant vector $\mathbf{v}_{i,G}$ for each target vector $\mathbf{x}_{i,G}$. This is achieved by adding the weighted difference between two randomly selected population vectors to a third vector. The most common mutation strategy, often referred to as DE/rand/1, is defined as:

$$\mathbf{v}_{i,G} = \mathbf{x}_{r1,G} + F \cdot (\mathbf{x}_{r2,G} - \mathbf{x}_{r3,G})$$

where $r1, r2, r3$ are distinct randomly chosen indices, and F is a scaling factor (typically $0 \leq F \leq 2$) that controls the amplification of the differential variation.

Crossover Crossover is the process of combining the mutant vector $\mathbf{v}_{i,G}$ with the target vector $\mathbf{x}_{i,G}$ to form a trial vector $\mathbf{u}_{i,G}$. The crossover operation helps to introduce diversity into the population. A commonly used crossover method is binomial (uniform) crossover:

$$u_{i,j,G} = \begin{cases} v_{i,j,G} & \text{if } \text{rand}_j(0,1) \leq CR \text{ or } j = j_{\text{rand}} \\ x_{i,j,G} & \text{otherwise} \end{cases}$$

where $u_{i,j,G}$ is the j-th component of the trial vector, CR is the crossover probability (typically $0 \leq CR \leq 1$), and j_{rand} is a randomly chosen index to ensure that at least one component of the trial vector differs from the target vector.

Selection Selection determines which vector (either the target vector $\mathbf{x}_{i,G}$ or the trial vector $\mathbf{u}_{i,G}$) will survive to the next generation. The trial vector replaces the target vector if it has a lower loss (or higher fitness, depending on the problem):

$$\mathbf{x}_{i,G+1} = \begin{cases} \mathbf{u}_{i,G} & \text{if } f(\mathbf{u}_{i,G}) \leq f(\mathbf{x}_{i,G}) \\ \mathbf{x}_{i,G} & \text{otherwise} \end{cases}$$

where $f(\cdot)$ is the objective function being minimized.

Termination The DE algorithm iterates through the mutation, crossover, and selection steps until a stopping criterion is met. Common termination criteria include reaching a maximum number of generations G_{max} or achieving a sufficiently low objective function value.

Advantages and Applications The DE algorithm is renowned for its simplicity, ease of implementation, and robustness in handling non-linear, non-differentiable, and multi-modal objective functions. It has been successfully applied in various domains such as engineering design, machine learning, and financial modeling. For a comprehensive overview of the Differential Evolution algorithm and its variants, readers are referred to the extensive literature on the subject [9].

2.2 Results with Differential Evolution

The Differential Evolution (DE) algorithm has provided optimized parameters for lens radii of 12 cm and 14 cm. It is evident from the table that, to achieve truly optimized parameter values, the iteration and population size need to be fairly large, specifically 60 and 16 respectively in our case. One notable point from Table 1 is the significantly lower loss observed with the 14 cm aperture radius.
Additionally, it is important to note that while we were expecting confocal solutions—where

the lens separation is twice the focal length—the solutions obtained from the optimizer can be classified as near-confocal. These are not true confocal solutions. Furthermore, Figure 1 shows that the maximum beam size is attained at the lens for the parameters resulting in minimum losses for a 12 cm radius aperture lens. This highlights the importance of accurately optimizing the beam parameters to achieve minimal loss.
The serrated aperture was introduced to study its effect on scattering and overall system performance. The optimization results for the serrated aperture are currently under review.

Run # (Lens radii)	**L_Lens (m)**	**Loss (ppm)**	**L focal (m)**	**w0 (mm)**	**z0 (m)**	**Pop size**	**Iters (max)**	**Pass**
Run 1 (12cm)	2061.44	2524	2432.5	33.7	-141.0	4	4.0	N/A
Run 2 (12cm)	3320.24	1465	2291.0	33.1	515.1	4	4.0	Fail
Run 3 (12cm)	3054.50	1302	1313.4	25.5	248.1	2	2.0	Fail
Run 4 (12cm)	3054.50	1302	1313.4	25.5	248.1	2	2.0	Fail
Run 5 (12cm)	2959.19	1921	3329.1	37.1	549.7	8	10.0	Fail
Run 6 (12cm)	3659.11	1309	2067.4	31.7	375.7	16	20.0	Fail
Run 7 (12cm)	3686.92	1102	1401.0	25.8	-47.7	16	40.0	Fail
Run 8 (12cm)	3750.09	1087	1453.9	26.2	-15.6	16	60.0	Pass
Run 9 (12cm)	3712.04	1088	1423.7	25.9	6.8	16	60.0	Fail
Run 10 (12cm)	3706.92	1087	1421.0	25.8	5.8	16	60.0	Fail
Run 11 (12cm)	3750.64	1086	1441.9	26.1	2.5	16	60.0	Pass
Run 12 (12cm)	3753.38	1087	1447.4	26.1	-12.0	16	60.0	Fail
Run 1 (14cm)	5002.80	796	1914.6	30.0	-12.3	16	60.0	Pass
Run 1* (14cm)	4622.18	883	1786.4	29.1	-10.6	16	60.0	Pass

Table 1: Optimization Results for Lens Array Parameters. The "Run" column indicates the number of iterations and lens radius used for each optimization attempt. The "Pass" column reflects the success flag from the SciPy library's differential evolution optimization process. A "Pass" value indicates that the algorithm successfully converged to a solution, with minimal changes in the objective function value between iterations, suggesting an optimal or near-optimal solution. "Run 1* (14cm)" denotes the use of a serrated aperture, while other runs use a circular non-serrated aperture.

3 Exploring the Parameter Space

To gain deeper insights into the parameter space, corner plots were generated for the four primary parameters: focal length, lens separation, w_0, and z_0. These plots illustrate the variations in photon loss across different parameter sets, offering a visual representation of the tolerance levels required for optimal operation in a vacuum beam guide. This analysis was performed using the Markov-Chain Monte Carlo (MCMC) algorithm with the `emcee` library and supporting tools.

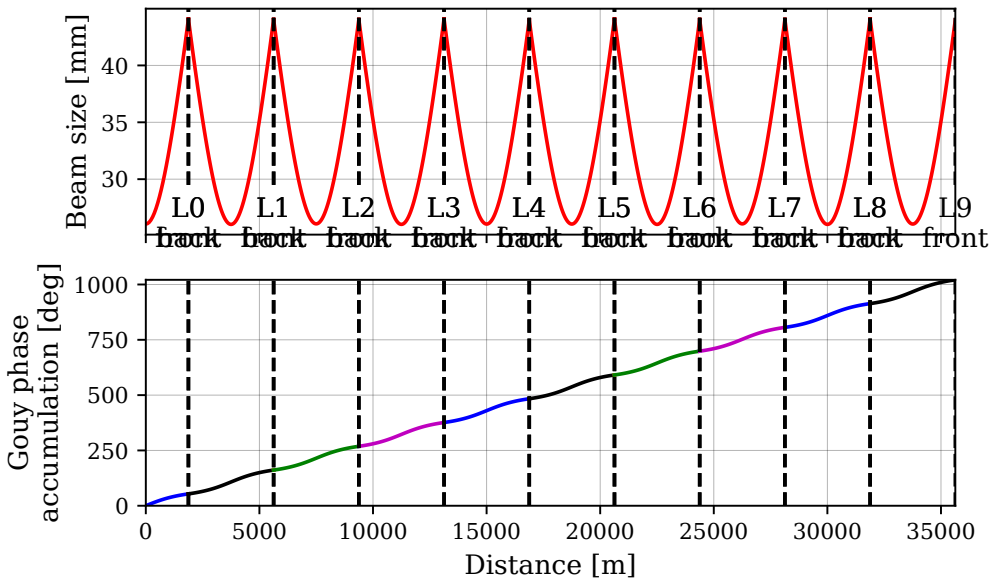

Figure 1: Plot of beam size and Gauy phase along the phase array Run 11 (12cm) in table 1

3.1 Markov-Chain Monte Carlo (MCMC) Algorithm

The Markov-Chain Monte Carlo (MCMC) algorithm is a powerful statistical tool used to sample from probability distributions by constructing a Markov chain that has the desired distribution as its equilibrium distribution. MCMC methods are particularly useful for high-dimensional problems where direct sampling is challenging. The key steps involved in the MCMC algorithm are as follows:

Initialization In the initialization step, an initial set of parameters θ_0 is selected. This initial state serves as the starting point for the Markov chain. The choice of the initial parameters can influence the convergence rate, but given sufficient iterations, the impact diminishes as the chain converges to the target distribution.

Proposal The proposal step involves generating new candidate parameters θ^* based on the current state θ_t of the chain. This is done using a proposal distribution $q(\theta^*|\theta_t)$, which suggests new states to explore. Common choices for the proposal distribution include Gaussian distributions centered at the current state, among others. The proposal step is formally expressed as:

$$\theta^* \sim q(\theta^*|\theta_t)$$

Acceptance The acceptance step decides whether to accept or reject the proposed candidate θ^*. This decision is based on the Metropolis-Hastings acceptance criterion, which ensures that the Markov chain converges to the target distribution $\pi(\theta)$. The acceptance probability α is given by:

$$\alpha = \min\left(1, \frac{\pi(\theta^*)q(\theta_t|\theta^*)}{\pi(\theta_t)q(\theta^*|\theta_t)}\right)$$

A uniform random number $u \sim \text{Uniform}(0, 1)$ is drawn, and the new state is accepted if $u \leq \alpha$:

$$\theta_{t+1} = \begin{cases} \theta^* & \text{if } u \leq \alpha \\ \theta_t & \text{otherwise} \end{cases}$$

Iteration The proposal and acceptance steps are iteratively repeated, allowing the chain to explore the parameter space. Over time, the distribution of the sampled states θ_t approaches the target distribution $\pi(\theta)$.

Burn-in and Convergence In practice, the initial samples from the chain (known as the burn-in period) are often discarded to ensure that the remaining samples are drawn from the stationary distribution. The length of the burn-in period depends on the problem and the initial state. Convergence diagnostics are employed to assess whether the chain has sufficiently mixed and reached equilibrium.

Applications and Advantages MCMC algorithms are widely used in Bayesian inference, where the goal is to estimate posterior distributions of parameters given observed data. They are also applicable in statistical physics, econometrics, and computational biology. The primary advantage of MCMC is its ability to handle complex, high-dimensional distributions that are difficult to sample using traditional methods. Detailed explanations and theoretical foundations of the MCMC algorithm can be found in statistical literature [10, 11].

3.2 Results from MCMC

The corner plots in Figure 2, generated from MCMC for a 12 cm lens radius, provide a comprehensive view of the parameter space. These plots illustrate how variations in each parameter affect the total photon losses and help identify the safe tolerance levels for each parameter to ensure optimal performance.

The corner plots indicate that the parameters w_0 and z_0 exhibit a narrower range of variation compared to the focal scale and lens separation. This observation is corroborated by the corner plot shown in Figure 2. It is crucial to pay special attention to the focal scale and lens separation when determining the optimal solution. The histograms for these parameters do not converge to a single point but rather display multiple regions where extremum points are located. This suggests that there are several subranges within the parameter space where optimal or near-optimal solutions can be found.

Understanding the distribution of these extremum points is essential for ensuring the robustness and reliability of the optimized parameters. The variability in the focal scale and lens separation indicates that multiple configurations can achieve minimal photon losses, highlighting the importance of thorough parameter space exploration to identify the most effective solutions. The exploration in this direction is in the process.

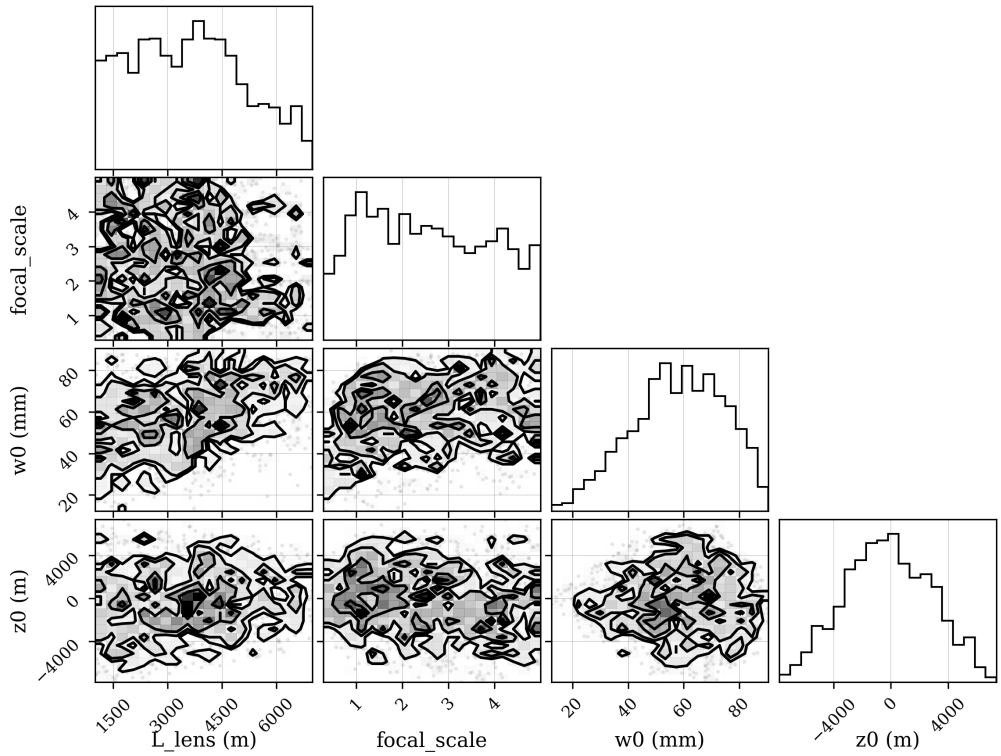

Figure 2: Corner Plot

4 Geophysical Analysis of Vacuum Beam Guide Design

It is imperative to conduct a geophysical study of possible Vacuum Beam Guide (VBG) designs. This study aims to address the impracticality of constructing a straight-line VBG over a distance of 4000 km due to the Earth's curvature. Placing the VBG underground is essential to shield it from environmental factors such as rain, high-speed winds, and potential theft in open areas.

Consider placing the VBG in a straight line between two points 4000 km apart on the Earth's surface. The following approximate analysis calculates the maximum depth required at the midpoint:

- Earth's radius $R \approx 6371$ km.
- Arc length s between the two points:

$$s = R\theta$$

  where θ is the central angle in radians.

- For an arc length of 4000 km:

$$\theta = \frac{s}{R} = \frac{4000\,\text{km}}{6371\,\text{km}} \approx 0.627\,\text{radians}$$

- Chord length d (straight-line distance between the two points):

$$d = 2R \sin\left(\frac{\theta}{2}\right)$$

$$d = 2 \times 6371 \times \sin\left(\frac{0.627}{2}\right) \approx 3987\,\text{km}$$

- Depth h required at the midpoint:

$$h = R - \sqrt{R^2 - \left(\frac{d}{2}\right)^2}$$

$$h = 6371 - \sqrt{6371^2 - \left(\frac{3987}{2}\right)^2} \approx 25.7\,\text{km}$$

This approximate analysis illustrates that a straight-line VBG over 4000 km would require digging approximately 25.7 km deep at the midpoint, which is impractical. Instead, constructing the VBG in smaller sections that follow the Earth's curvature is necessary.

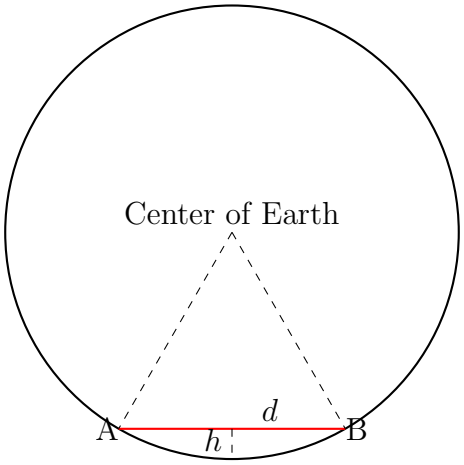

Figure 3: Illustration of the impractical depth required for a straight-line Vacuum Beam Guide (VBG) over 4000 km.

References

[1] S. Wehner, D. Elkouss, R. Hanson, *Quantum internet: A vision for the road ahead*, *Science* **362**(6412), eaam9288 (2018).

[2] A. W. Goodwin-Jones, R. Cabrita, M. Korobko, M. Van Beuzekom, D. D. Brown, V. Fafone, J. Van Heijningen, A. Rocchi, M. G. Schiworski, M. Tacca, *Transverse mode control in quantum enhanced interferometers: a review and recommendations for a new generation*, *Optica* **11**(2), 273-290 (2024).

[3] H. Sakr, T. D. Bradley, G. T. Jasion, E. N. Fokoua, S. R. Sandoghchi, I. A. Davidson, A. Taranta, G. Guerra, W. Shere, Y. Chen, et al., *Hollow core NANFs with five nested tubes and record low loss at 850, 1060, 1300 and 1625nm*, *Optical Fiber Communication Conference*, F3A-4 (2021).

[4] D. Gottesman, T. Jennewein, S. Croke, *Longer-baseline telescopes using quantum repeaters*, *Physical Review Letters* **109**, 070503 (2012).

[5] Y. Huang, R. X. Adhikari, A. H. Safavi-Naeini, L. Jiang, et al., *Vacuum Beam Guide for Large-Scale Quantum Networks*, *arXiv preprint arXiv:2312.09372* (2023).

[6] R. Storn, K. Price, *Differential evolution–a simple and efficient adaptive scheme for global optimization over continuous spaces*, *International Computer Science Institute*, (1995).

[7] N. Sangouard, C. Simon, H. De Riedmatten, N. Gisin, *Quantum repeaters based on atomic ensembles and linear optics*, *Reviews of Modern Physics* **83**(1), 33 (2011).

[8] S. Goswami, S. Dhara, *Satellite-relayed global quantum communication without quantum memory*, *Physical Review Applied* **20**(2), 024048 (2023).

[9] R. Storn, K. Price, *Differential evolution–a simple and efficient heuristic for global optimization over continuous spaces*, *Journal of Global Optimization* **11**, 341–359 (1997).

[10] W. R. Gilks, S. Richardson, D. Spiegelhalter, *Markov chain Monte Carlo in practice*, CRC Press (1995).

[11] S. Brooks, A. Gelman, G. Jones, X.-L. Meng, *Handbook of Markov Chain Monte Carlo*, CRC Press (2011).